 CMC, vol.23, no.3, pp.187-199, 2011

Effect of Electric Field on the Response of Clamped-Free Magnetostrictive/Piezoelectric/Magnetostrictive Laminates

Kotaro Mori[1], **Fumio Narita**[1] **and Yasuhide Shindo**[1]

Abstract: This work deals with the response of clamped-free magnetostrictive/piezoelectric/magnetostrictive laminates under electric field both numerically and experimentally. The laminate is fabricated using two magnetostrictive Terfenol-D layers and a soft piezoelectric PZT layer. Easy axis of Terfenol-D layers is length direction, while the polarization of PZT layer is the thickness direction. The magnetostriction of the Terfenol-D layers bonded to the upper and lower surfaces of the PZT layer is first measured. Next, a nonlinear finite element analysis is employed to evaluate the second-order magnetoelastic constants in the Terfenol-D layers bonded to the PZT layer using measured data. The induced magnetic field and internal stresses for the laminates under electric field parallel to the poling are then calculated and discussed in detail. In addition, the induced magnetic field is measured, and test results are presented to validate the predictions.

Keywords: magnetostrictive/piezoelectric mechanics, electronic laminates, detection and response characteristics

1 Introduction

Magnetostrictive alloys and piezoelectric ceramics are an important branch of modern engineering materials, with wide applications in sensors and actuators in smart materials and structures. $Tb_{0.3}Dy_{0.7}Fe_2$ (Terfenol-D) is a highly magnetostrictive alloy of iron and rare-earth metals, and has a unique advantage over the other functional materials and structures. In particular, Terfenol-D has outstanding elongation and energy density at room temperature. In recent years, it has been found that the magnetostrictive Terfenol-D and piezoelectric PZT laminated composites possess superior magnetoelectric (ME) effect. The Terfenol-D/piezoelectric/Terfenol-D laminated composites are recognized for the potential utility in applications in coil-free magnetic-sensitive sensors [Jia et al 2006a, Record et al 2007]. These

[1] Tohoku University , Sendai, Japan.

sensors are applied for example to magnetic (dc or quasi-dc) anomaly detection. Recently, Popov et al. [2008] prepared laminar Terfenol-D/PZT/Terfenol-D and PZT/Terfenol-D/PZT composites, and measured the direct and converse ME coefficients in the trilayer composites. Lu et al. [2008] also prepared Terfenol-D/piezoelectric/Terfenol-D systems, and examined the dielectric permittivity of the layered systems under magnetic field.

The electric-field-induced magnetization has technical applications such as coil-free magnetic levitation and step motor [Ueno and Higuchi 2006], and understanding of converse ME effect of the trilayer composites is necessary. Though many researches on the direct ME effect of the trilayer composites are found in the literature, the investigations on the characterization of the converse ME effect are few [Porov et al 2008]. Also, many works were restricted to the ME effect and did not consider the mechanical behavior; this viewpoint is important for the design of long-life magnetostrictive/piezoelectric/magnetostrictive laminated composites.

In this work, we investigate the response of clamped-free magnetostrictive/piezoelectric/magnetostrictive laminates under electric field in a combined numerical and experimental approach. The fabricated laminates consist of thin Terfenol-D and soft PZT layers. Easy axis of Terfenol-D layers and polarization of PZT layer are length and thickness directions, respectively. The magnetostriction of the Terfenol-D layers bonded to the upper and lower surfaces of the PZT layer was measured, and the second-order magnetoelastic constant was evaluated based on the nonlinear finite element method using measured data. The induced magnetic field and internal stresses for the Terfenol-D/PZT/Terfenol-D laminates under electric field were then predicted and examined. In addition, the induced magnetic field was measured, and a comparison was made between experiment and simulation.

2 Analysis

2.1 Basic equations

The basic equations for magnetostrictive and piezoelectric materials are outlined here. Consider the rectangular Cartesian coordinate system O-$x_1x_2x_3$. The equilibrium equations are given by

$$\sigma_{ji,j} = 0 \tag{1}$$

$$B_{i,i} = 0 \tag{2}$$

$$D_{i,i} = 0 \tag{3}$$

where σ_{ij} is the stress tensor, B_i is the magnetic induction vector, D_i is the electric displacement vector, a comma followed by an index denotes partial differentiation

with respect to the space coordinate x_i, and the summation convention for repeated tensor indices is applied. The constitutive laws are given as follows:

$$\varepsilon_{ij} = s^H_{ijkl}\sigma_{kl} + d'_{kij}H_k \tag{4}$$

$$B_i = d'_{ikl}\sigma_{kl} + \mu_{ik}H_k \tag{5}$$

for the magnetostrictive, and

$$\varepsilon_{ij} = s^E_{ijkl}\sigma_{kl} + d_{kij}E_k \tag{6}$$

$$D_i = d_{ikl}\sigma_{kl} + \kappa^T_{ik}E_k \tag{7}$$

for the piezoelectric. Here, ε_{ij} is the strain tensor, H_i is the magnetic field intensity vector, E_i is the electric field intensity vector, $s^H_{ijkl}, d'_{kij}, \mu_{ij}$ are the constant magnetic field elastic compliance, magnetoelastic constant and magnetic permittivity of magnetostrictive material, and $s^E_{ijkl}, d_{kij}, \kappa^T_{ij}$ are the constant electric field elastic compliance, direct piezoelectric constant and dielectric permittivity of piezoelectric material. Valid symmetry conditions for the material constants are

$$s^H_{ijkl} = s^H_{jikl} = s^H_{ijlk} = s^H_{klij}, \;\; d'_{kij} = d'_{kji}, \;\; \mu_{ij} = \mu_{ji} \tag{8}$$

$$s^E_{ijkl} = s^E_{jikl} = s^E_{ijlk} = s^E_{klij}, \;\; d_{kij} = d_{kji}, \;\; \kappa^T_{ij} = \kappa^T_{ji} \tag{9}$$

The relation between the strain tensor and the displacement vector u_i is given by

$$\varepsilon_{ij} = \frac{1}{2}(u_{j,i} + u_{i,j}) \tag{10}$$

The magnetic and electric field intensities are written as

$$H_i = \varphi_{,i} \tag{11}$$

$$E_i = -\phi_{,i} \tag{12}$$

where φ and ϕ are the magnetic and electric potentials, respectively.

2.2 Model

A three-layered magnetostrictive/piezoelectric/magnetostrictive laminate is shown in Figure 1, in which magnetostrictive layers, Terfenol-D, of length l_m = 15 mm, width w_m = 5 mm and thickness h_m = 1, 3, 5 mm are perfectly bonded on the upper and lower surfaces of a piezoelectric layer, PZT, of length l_p = 20 mm, width w_p = 5

mm and thickness $h_p = 0.5$ mm. We will use subscripts m and p to refer to Terfenol-D and PZT layers, respectively. Dimensions $h_m(h_p)$, $w_m(w_p)$, $l_m(l_p)$ are measured along the $x_1 = x$, $x_2 = y$ and $x_3 = z$ axis, respectively. The origin of the coordinate system is located at the center of the bottom left side of upper Terfenol-D layer, and the left end $z = 0$ is clamped. Easy axis of the magnetization of Terfenol-D layers is the z-direction, while the polarization of PZT layer is the x-direction. The constitutive relations for Terfenol-D and PZT layers are given by Appendix A.

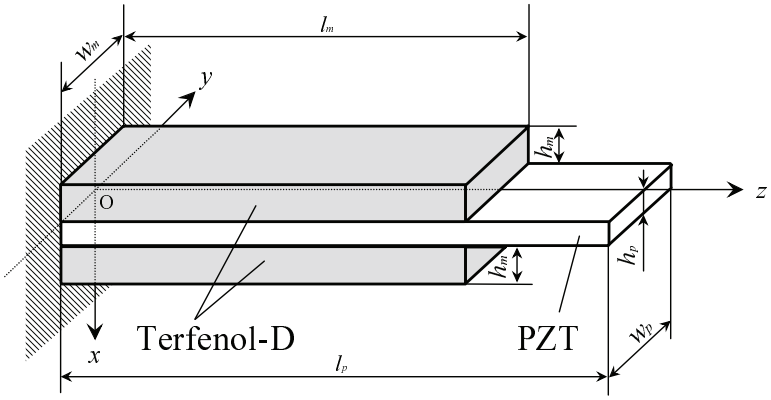

Figure 1: Illustration of Terfenol-D/PZT/Terfenol-D laminate configuration

As we know, nonlinearity of magnetostriction vs magnetic filed curves arises from the rotation of magnetic domains [Wan et al 2003]. A magnetic domain switching gives rise to the changes of the magnetoelastic constants, and the constants d'_{15}, d'_{31} and d'_{33} for Terfenol-D layer under a uniform magnetic field of magnetic induction $B_z = B_0$ are

$$\begin{aligned} d'_{15} &= d^m_{15} \\ d'_{31} &= d^m_{31} + m_{31} H_z \\ d'_{33} &= d^m_{33} + m_{33} H_z \end{aligned} \tag{13}$$

where $d^m_{15}, d^m_{31}, d^m_{33}$ are the piezo-magnetic constants, and m_{31} and m_{33} are the second-order magnetoelastic constants. When the length of Terfenol-D is much longer than other two sizes (width and thickness) and a magnetic field is along the length direction (easy axis), the longitudinal (33) magnetostrictive deformation mode is dominant. So it is assumed that only the constant d'_{33} varies with magnetic field H_z, and the constant m_{31} equals to zero. The constant m_{33} can predict well the nonlinearity, without complex computation and more parameters [Jia et al 2006b].

More realistic material models are much more complicated, see e.g. [Linnemann et al 2009], but the present formulation is able to capture the nonlinear effect, which

is a remarkable feature of the presented model. The output (nonlinear strain versus magnetic field curve) is known from experiments while the additional parameter m_{33} need to be determined. This requires the finite element analysis (FEA) be done in an inverse way where iteration of finite element simulation is performed to find the constitutive properties that give the best much between the simulated and experimental outputs.

We performed finite element calculations to obtain the strain, internal stress and induced magnetic field for the Terfenol-D/PZT/Terfenol-D laminates. The electric potential on the $x = 0$ plane of PZT layer equals the applied voltage $\phi = V_0$. The $x = h_p$ plane is connected to the ground, so that $\phi = 0$. The average induced magnetic field in the z-direction at the side surface (at $z = l_m$ plane) of each Terfenol-D layer is calculated as

$$B_{\text{in}} = \frac{1}{A}\int_A B_z(x, y, l_m)dA \tag{14}$$

where the integration is over the surface area, $A = w_m h_m$, of the Terfenol-D layer. The basic equations for the magnetostrictive materials are mathematically equivalent to those for piezoelectric materials. So eight-node 3D coupled-field solid elements in ANSYS were used in the analysis. The FEA was performed using the model with the epoxy-bond layer, but the epoxy-bond layer did not affect the general results (not shown here). In total, 4300, 10300 and 16300 elements and 5568, 13008 and 20448 nodes were used for h_m = 1, 3 and 5 mm, respectively. It should be noted that before carrying out simulations, a mesh sensitivity study was performed to ensure that the mesh was fine enough.

From the third of Equations (13), the magnetoelastic constant d'_{33} varies with magnetic field. Making use of magnetic field dependent material properties, the model calculated the nonlinear behavior. The finite element computations were provided by modifying the program with routines developed by our previous work [Shindo et al 2009, 2010].

3 Experimental Procedures

Terfenol-D (Etrema Products, Inc., USA) of l_m = 15 mm, w_m = 5 mm and h_m = 1, 3, 5 mm and PZT C-91 (Fuji Ceramics, Co. Ltd., Japan) of l_p = 20 mm, w_p = 5 mm and h_p = 0.5 mm were used to make magnetostrictive/piezoelectric/magnetostrictive laminates by epoxy bonding (EP-34B; Kyowa Electronic Instruments Co. Ltd., Japan). The thickness of the epoxy layer is about 50 μm. Table 1 and Table 2 list the material properties of Terfenol-D [Engdahl 2000, Nan et al 2001] and C-91 [Narita et al 2005], respectively.

Table 1: Material properties of Terfenol-D

	Elastic compliance ($\times 10^{-12}$m^2/N)					Piezo-magnetic constant ($\times 10^{-9}$m/A)			Magnetic permittivity ($\times 10^{-6}$H/m)	
	s_{11}^H	s_{33}^H	s_{44}^H	s_{12}^H	s_{13}^H	d_{31}^m	d_{33}^m	d_{15}^m	μ_{11}	μ_{33}
Terfenol-D	17.9	17.9	26.3	−5.88	−5.88	−5.3	11	28	6.29	6.29

Table 2: Material properties of PZT

	Elastic compliance ($\times 10^{-12}$m^2/N)					Direct piezoelectric constant ($\times 10^{-12}$m/V)			Dielectric permittivity ($\times 10^{-10}$C/Vm)	
	s_{11}^E	s_{33}^E	s_{44}^E	s_{12}^E	s_{13}^E	d_{31}	d_{33}	d_{15}	κ_{11}^T	κ_{33}^T
C-91	17.1	18.6	41.4	−6.3	−7.3	−340	645	836	395	490

Figure 2 shows the setup for the experiment of Terfenol-D/PZT/Terfenol-D laminates. First, a strain gage was placed at the center of the surface ($x = -h_m$, $y = 0$, $z = l_m/2$) in upper Terfenol-D layer. Magnetic field was then applied in the z- direction, and the magnetostriction was evaluated (see Fig. 2(a)). Next, the induced magnetic field over the total area on $z = l_m$ plane of upper Terfenol-D in the laminate under electric field was measured using a Tesla meter (see Fig.2(b)). Voltage V_0 was applied to the $x = 0$ plane of PZT layer, whereas the $x = h_p$ plane was grounded.

4 Results and discussion

Figure 3 shows the strain ε_{zz} versus magnetic field B_0 at $x = -h_m$, $y = 0$ mm and $z = 7.5$ mm for the Terfenol-D/PZT/Terfenol-D laminates with h_m = 1, 3, 5 mm. The lines and plots denote the results of nonlinear FEA and test, respectively. The strain was evaluated at the nodal point, and this was fitted to the location of the experimental measurement (center of the strain gage). A nonlinear relationship between strain and magnetic field is observed, and the constants m_{33} of Terfenol-D layer with h_m = 1, 3, 5 mm are 5.2 $\times 10^{-12}$, 2.3 $\times 10^{-12}$, 1.7 $\times 10^{-13}$ m^2/A^2, respectively. Figure 4 shows the average induced magnetic field B_{in} versus applied electric field $E_0 = V_0 / h_p$ for the Terfenol-D/PZT/Terfenol-D laminates with h_m = 1, 3, 5 mm obtained from the FEA. Also shown are the measured data for h_m = 3 and 5 mm. The comparison between the FEA and test is reasonable for h_m = 5 mm. For h_m = 3 mm, the measured data are little larger than the calculated data. As the electric field increases, the induced magnetic field increases. The induced magnetic field also increases as the thickness of the Terfenol-D layers decreases.

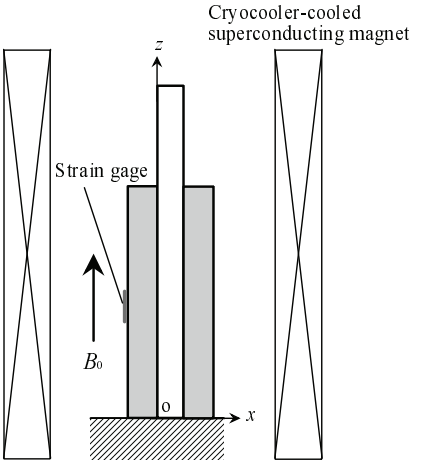

(a)

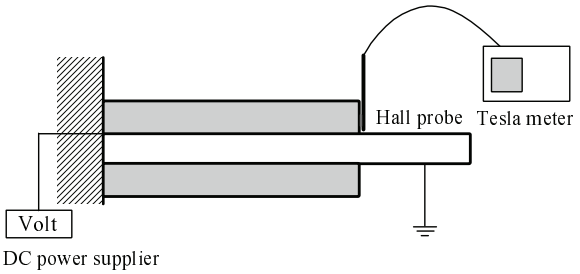

(b)

Figure 2: Experimental setup for measuring (a) the magnetostriction and (b) the induced magnetic field

The variations of normal stress σ_{zz} along the thickness direction are calculated at a chosen point ($y = 0$ mm and $z = 7.5$ mm here) for the Terfenol-D/PZT/Terfenol-D laminates and the results are shown in Figure 5. The observation point corresponds to the mid-width line of the mid-length plane for the Terfenol-D layer. All calculations were done, for example, at a fixed average induced magnetic field of B_{in}= 0.2 mT. The applied electric fields of PZT layer at B_{in}= 0.2 mT are about E_0 = 0.13, 0.22, 0.27 MV/m for $h_m = 1,3,5$ mm, respectively. There are some stress gaps at the interface between Terfenol-D and PZT layers as is expected. At smaller Terfenol-D layer thickness, lower stress gap is found for the same average induced

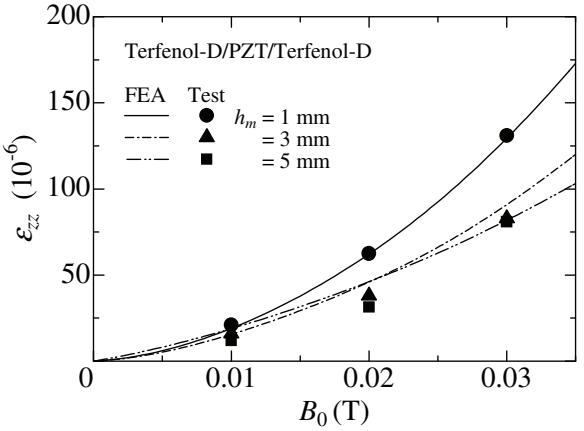

Figure 3: Strain versus magnetic field at $x = -h_m$, $y = 0$ mm and $z = 7.5$ mm for Terfenol-D/PZT/Terfenol-D laminates

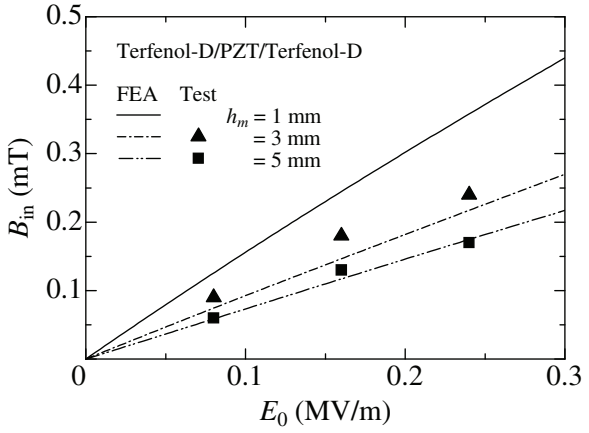

Figure 4: Average induced magnetic field versus electric field at $z = 15$ mm plane of upper Terfenol-D layer for Terfenol-D/PZT/Terfenol-D laminates

magnetic field. In the case of other average induced magnetic fields, similar results can be predicted. Figure 6 shows the variations of shear stress σ_{xz} along the length direction at $x = y = 0$ mm for the Terfenol-D/PZT/Terfenol-D laminates at B_{in}= 0.2 mT. High shear stress is observed near the side surface for each laminate. Low shear stress is noted for small Terfenol-D layer thickness at the same average induced magnetic field. The results for the evaluation of internal stresses may help Terfenol-D/PZT/Terfenol-D laminate designers to optimize in-service loading conditions.

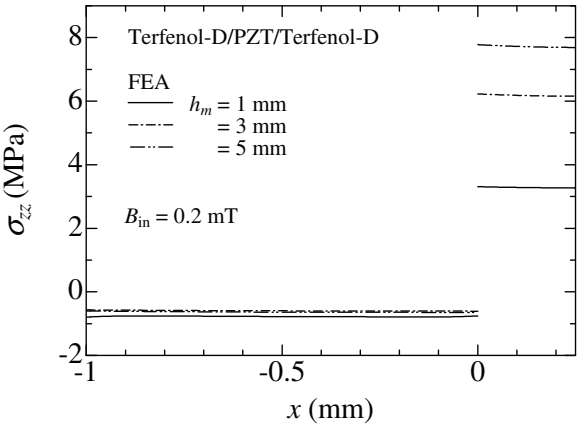

Figure 5: Normal stress distribution along the thickness direction at $y = 0$ and $z = 7.5$ mm for Terfenol-D/PZT/Terfenol-D laminates

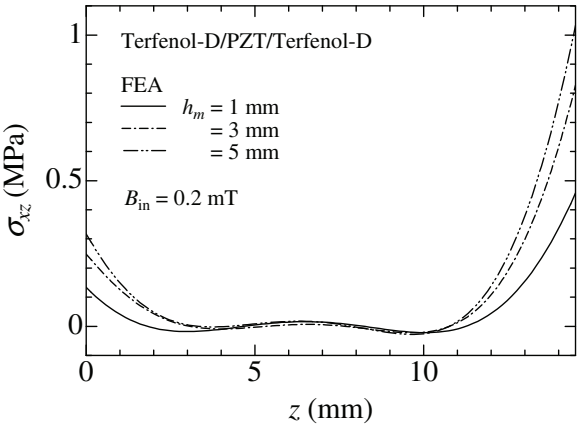

Figure 6: Shear stress distribution along the length direction at $x = 0$ and $y = 0$ mm for Terfenol-D/PZT/Terfenol-D laminates

5 Conclusions

Numerical and experimental approaches have been presented to characterize the electromagneto-mechanical fields in clamped-free magnetostrictive/piezoelectric/-magnetostrictive laminates under electric fields. The average induced magnetic field is predicted using finite element simulations, and comparison with the measured data shows that current predictions are reasonable. It was found that the average induced magnetic field depends on the magnetostrictive layer thickness. Also,

smaller magnetostrictive layer thickness gave smaller internal stresses for the same average induced magnetic field of the laminates due to electric field. This study may be useful in designing the long-life magnetostrictive/piezoelectric/magnetostrictive laminates.

Acknowledgement: This work was supported by Global Center of Excellence (COE) Program "Materials Integration (International Center of Education and Research), Tohoku University", Ministry of Education, Culture, Sports, Science and Technology, Japan.

References

Engdahl, G. (2000): *Handbook of Giant Magnetostrictive Materials*. Academic Press.

Jia, Y.; Tang, Y.; Zhao, X.; Luo, H.; Or, S. W.; Chan, H. L. W. (2006a): Additional dc magnetic field response of magnetostrictive/piezoelectric magnetoelectric laminates by Lorentz force effect. *J. Appl. Phys.*, vol. 100, 126102.

Jia, Z.; Liu, W.; Zhang, Y.; Wang, F.; Guo, D. (2006b): A nonlinear magnetomechanical coupling model of giant magnetostrictive thin films at low magnetic fields. *Sens. Actuators A*, vol. 128, pp. 158–164

Linnemann, K.; Klinkel, S.; Wagner, W. (2009): A constitutive model for magnetostrictive and piezoelectric materials. *Int. J. Solids Struct.*, vol. 46, pp. 1149–1166

Lu, X.; Wang, B.; Zheng, Y.; Liu, Y.; Li, C. (2008): Magnetic control of dielectric properties of $Ba_{0.6}Sr_{0.4}TiO_3$ in a trilayer system. *J. Phys. D Appl. Phys.*, vol. 41, 095004

Nan, C. W.; Li, M.; Huang, J. H. (2001): Calculations of giant magnetoelectric effects in ferroic composites of rare-earth-iron alloys and ferroelectric polymers. *Phys. Rev. B*, vol. 63, 144415

Narita, F.; Shindo, Y.; Hayashi, K. (2005): Bending and polarization switching of piezoelectric laminated actuators under electromechanical loading. *Comput. Struct.*, vol. 83, pp. 1164–1170

Popov, C.; Chang, H.; Record, P. M.; Abraham, E.; Whatmore, R. W.; Huang, Z. (2008): Direct and converse magnetoelectric effect at resonant frequency in laminar piezoelectric-magnetostrictive composite. *J. Electroceramics*, vol. 20, pp. 53–58

Record, P.; Popov, C.; Fletcher, J.; Abraham, E.; Huang, Z.; Chang, H.; Whatmore, R. W. (2007): Direct and converse magnetoelectic effect in laminate bonded

Terfenol-D–PZT composites. *Sens. Actuators B*, vol. 126, pp. 344–349

Shindo, Y.; Narita, F.; Mori, K.; Nakamura, T. (2009): Nonlinear bending response of giant magnetostrictive laminated actuators in magnetic fields. *J. Mech. Mater. Struct.*, vol. 4, pp. 941–949

Shindo, Y.; Mori, K.; Narita, F. (2010): Electromagneto-mechanical fields of giant magnetostrictive/piezoelectric laminates. *Acta Mech.*, vol. 212, pp. 253–261

Ueno, T.; Higuchi, T. (2006): Novel composite of magnetostrictive material and piezoelectric actuator for coil-free magnetic force control. *Sens. Actuators A*, vol. 129, pp. 251–255

Wan, Y.; Fang, D.; Hwang, K.-C. (2003): Non-linear constitutive relations for magnetostrictive materials. *Int. J. Non-Linear Mech.*, vol. 38, pp. 1053–1065

Appendix A:

For Terfenol-D, the constitutive relations can be written in the following form:

$$\begin{Bmatrix} \varepsilon_{xx} \\ \varepsilon_{yy} \\ \varepsilon_{zz} \\ \varepsilon_{yz} \\ \varepsilon_{zx} \\ \varepsilon_{xy} \end{Bmatrix} = \begin{bmatrix} s_{11}^H & s_{12}^H & s_{13}^H & 0 & 0 & 0 \\ s_{12}^H & s_{11}^H & s_{13}^H & 0 & 0 & 0 \\ s_{13}^H & s_{13}^H & s_{33}^H & 0 & 0 & 0 \\ 0 & 0 & 0 & s_{44}^H/2 & 0 & 0 \\ 0 & 0 & 0 & 0 & s_{44}^H/2 & 0 \\ 0 & 0 & 0 & 0 & 0 & s_{66}^H/2 \end{bmatrix} \begin{Bmatrix} \sigma_{xx} \\ \sigma_{yy} \\ \sigma_{zz} \\ \sigma_{yz} \\ \sigma_{zx} \\ \sigma_{xy} \end{Bmatrix} + \begin{bmatrix} 0 & 0 & d'_{31} \\ 0 & 0 & d'_{31} \\ 0 & 0 & d'_{33} \\ 0 & d'_{15}/2 & 0 \\ d'_{15}/2 & 0 & 0 \\ 0 & 0 & 0 \end{bmatrix} \begin{Bmatrix} H_x \\ H_y \\ H_z \end{Bmatrix} \quad (15)$$

$$\begin{Bmatrix} B_x \\ B_y \\ B_z \end{Bmatrix} = \begin{bmatrix} 0 & 0 & 0 & 0 & d'_{15} & 0 \\ 0 & 0 & 0 & d'_{15} & 0 & 0 \\ d'_{31} & d'_{31} & d'_{33} & 0 & 0 & 0 \end{bmatrix} \begin{Bmatrix} \sigma_{xx} \\ \sigma_{yy} \\ \sigma_{zz} \\ \sigma_{yz} \\ \sigma_{zx} \\ \sigma_{xy} \end{Bmatrix} + \begin{bmatrix} \mu_{11} & 0 & 0 \\ 0 & \mu_{11} & 0 \\ 0 & 0 & \mu_{33} \end{bmatrix} \begin{Bmatrix} H_x \\ H_y \\ H_z \end{Bmatrix} \quad (16)$$

where

$$\left.\begin{array}{l} s_{11}^H = s_{1111}^H = s_{2222}^H,\ s_{12}^H = s_{1122}^H,\ s_{13}^H = s_{1133}^H = s_{2233}^H,\ s_{33}^H = s_{3333}^H \\ s_{44}^H = 4s_{2323}^H = 4s_{3131}^H,\ s_{66}^H = 4s_{1212}^H = 2(s_{11}^H - s_{12}^H) \end{array}\right\} \tag{17}$$

$$d'_{15} = 2d'_{131} = 2d'_{223},\ \ d'_{31} = d'_{311} = d'_{322},\ \ d'_{33} = d'_{333} \tag{18}$$

The constitutive relations for PZT (hexagonal crystal of class 6mm) are

$$\begin{Bmatrix} \varepsilon_{xx} \\ \varepsilon_{yy} \\ \varepsilon_{zz} \\ \varepsilon_{yz} \\ \varepsilon_{zx} \\ \varepsilon_{xy} \end{Bmatrix} = \begin{bmatrix} s_{33}^E & s_{13}^E & s_{13}^E & 0 & 0 & 0 \\ s_{13}^E & s_{11}^E & s_{12}^E & 0 & 0 & 0 \\ s_{13}^E & s_{12}^E & s_{11}^E & 0 & 0 & 0 \\ 0 & 0 & 0 & s_{66}^E/2 & 0 & 0 \\ 0 & 0 & 0 & 0 & s_{44}^E/2 & 0 \\ 0 & 0 & 0 & 0 & 0 & s_{44}^E/2 \end{bmatrix} \begin{Bmatrix} \sigma_{xx} \\ \sigma_{yy} \\ \sigma_{zz} \\ \sigma_{yz} \\ \sigma_{zx} \\ \sigma_{xy} \end{Bmatrix} + \begin{bmatrix} d_{33} & 0 & 0 \\ d_{31} & 0 & 0 \\ d_{31} & 0 & 0 \\ 0 & 0 & 0 \\ 0 & 0 & d_{15}/2 \\ 0 & d_{15}/2 & 0 \end{bmatrix} \begin{Bmatrix} E_x \\ E_y \\ E_z \end{Bmatrix} \tag{19}$$

$$\begin{Bmatrix} D_x \\ D_y \\ D_z \end{Bmatrix} = \begin{bmatrix} d_{33} & d_{31} & d_{31} & 0 & 0 & 0 \\ 0 & 0 & 0 & 0 & 0 & d_{15} \\ 0 & 0 & 0 & 0 & d_{15} & 0 \end{bmatrix} \begin{Bmatrix} \sigma_{xx} \\ \sigma_{yy} \\ \sigma_{zz} \\ \sigma_{yz} \\ \sigma_{zx} \\ \sigma_{xy} \end{Bmatrix} + \begin{bmatrix} \kappa_{33}^T & 0 & 0 \\ 0 & \kappa_{11}^T & 0 \\ 0 & 0 & \kappa_{11}^T \end{bmatrix} \begin{Bmatrix} E_x \\ E_y \\ E_z \end{Bmatrix} \tag{20}$$

where

$$\left.\begin{array}{l} s_{11}^E = s_{2222}^E = s_{3333}^E,\ s_{12}^E = s_{2233}^E,\ s_{13}^E = s_{1122}^E = s_{1133}^E,\ s_{33}^E = s_{1111}^E \\ s_{44}^E = 4s_{1212}^E = 4s_{1313}^E,\ s_{66}^E = 4s_{2323}^E = 2(s_{11}^E - s_{12}^E) \end{array}\right\} \tag{21}$$

$$d_{15} = 2d_{313} = 2d_{212},\ \ d_{31} = d_{122} = d_{133},\ \ d_{33} = d_{111} \tag{22}$$